Distinguishing dispersion from distributed scattering in S^2 fiber mode analysis

J. Jasapara*, A. D. Yablon

Interfiber Analysis, LLC, 26 Ridgewood Drive, Livingston, NJ 07039

ABSTRACT

We introduce a new spectrogram approach for analyzing spatially- and spectrally-resolved interferometry (S^2) data that overcomes the previously overlooked ambiguity between dispersion and distributed scattering. Traditionally, S^2 yields a one-dimensional spectrum of inter-modal group delays between higher-order-modes (HOMs) and the dominant fundamental mode. According to this interpretation, inter-modal group delay broadening is considered to be a location signature of HOM scattering; for example, a narrow peak in the spectrum is interpreted to be a discrete scattering event whereas a broad feature is interpreted to be distributed scattering along the fiber. Since the inter-modal dispersion is high for weakly guided HOMs, discrete scattering events will also manifest as broadened features. For the first time, we demonstrate a spectrogram approach to S^2 analysis in which the spectral interference data is analyzed over small staggered wavelength windows and the inter-modal group delay is plotted as a function of wavelength. In this new two-dimensional map the wavelength dependence of the inter-modal group delay produces an inclination of streaks traversing the spectrogram. This new perspective resolves the ambiguity as to whether group delay broadening is caused by fiber dispersion or distributed scattering that is inherent to the previous one-dimensional S^2 mapping. The spectrogram is a more accurate map of mode conversion along the fiber length and is essential for evaluating high power fibers and devices. Results for standard telecom single mode fiber and a large-mode-area fiber are presented.

Keywords: Fiber mode characterization, Multimode fibers, fiber lasers and amplifiers, intermodal dispersion

1. INTRODUCTION

Propagation of high intensities in optical fibers often requires the use of large-mode-area (LMA) fibers to mitigate nonlinear distortions in the signal. These fibers support higher-order-modes (HOM) besides the fundamental mode. Even though care is taken at the fiber input to primarily excite the fundamental mode, residual light usually gets coupled into the HOM, either due to a perturbation of the fiber at a discreet location, or due to a distributed perturbation along the fiber length. This excitation of HOM is undesirable because they distort the beam at the fiber output and may cause beam pointing instability. It is therefore necessary to characterize the modal content at the fiber output and determine the cause and location of the perturbation causing the coupling into the HOM.

In the past the M^2 parameter was widely used to characterize the beam quality. However it has been shown that multiple modes can interfere at the output resulting in an unstable M^2 which may lead to an erroneous impression about the beam quality[1]. Recently the techniques of (i) spatially-resolved-spectral-interferometry[2-4] (S^2), and (ii) cross-correlation interferometry[5] (C^2), have been demonstrated as alternatives to characterize fiber modal content. The spatially resolved spectral interferometry technique to characterize the energy exchanged between modes in multi-mode fibers is based on measuring the inter-modal group delay between the various guided modes and a dominant fundamental mode. S^2 is powerful not only because it provides the relative power and spatial distribution of the excited modes, but also because it provides insight into whether those modes are excited at discrete or distributed locations within the fiber. This diagnosis can be acted upon to improve the fiber design, excitation, and packaging. For this reason, S^2 is an important tool to evaluate fibers used in fiber lasers/amplifiers[6,8], sensors, or telecom systems[7].

A narrow spike in the S^2 intermodal group delay spectrum indicates a discrete excitation of a higher-order-mode. Whereas a broad distribution in inter-modal group delay was previously[2] assumed to be distributed mode excitation in the fiber. These early studies ignored the effects of intermodal dispersion on the measurement. We discovered that the fiber's dispersion can cause a discrete scattering event to manifest itself as a broad distribution in the intermodal group delay[9]. This is especially the case in fibers designed for lasers that have low numerical-apertures and weakly guide HOMs with strong waveguide dispersion.

In this paper we demonstrate the significant effect of intermodal dispersion on the S^2 spectrum. The signature of intermodal dispersion is revealed by a new approach to S^2 data analysis which resolves the ambiguity associated with broadened distributions in the intermodal group delay maps. In our approach the data is analyzed over small staggered wavelength windows across the measurement bandwidth and assembled together to form a map of the intermodal group delay as a function of wavelength – we call this map a *spectrogram*. The wavelength dependence of the intermodal group delay manifests itself as an inclination in streaks traversing the spectrogram. This new two-dimensional perspective resolves the ambiguity as to whether group delay broadening is caused by fiber dispersion or distributed scattering that is inherent to the previous one-dimensional S^2 mapping[2-4]. Results for a standard telecom single mode fiber and a large-mode-area (LMA) fiber are presented.

Recently a sliding window approach to S^2 analysis was independently proposed[10], however in their technique the spatial dependence of the intermodal interference is lost and therefore they are unable to identify the modes corresponding to the various spectrogram trajectories. In contrast our technique preserves the spatial dependence of the interference and the spectrogram provides direct identification of the modes.

2. EXPERIMENT

2.1 Experimental Setup

Figure 1 shows the experimental setup used in our S^2 measurement. A narrow line-width laser (line-width ≤ 130 kHz) tunable from 1000 nm to 1066 nm is launched into the fiber under test. The output end of this fiber is imaged onto a silicon CCD camera which captures the near-field images as the laser wavelength is scanned across its ~66 nm span. The camera pixel size was approximately 6×6 μm. A 100×100 pixel area was sufficient to capture the magnified near field images.
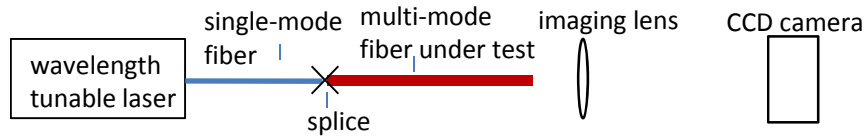

Fig. 1: Schematic of experimental setup.

The laser output is attenuated and effectively polarized by two reflections off glass wedges near Brewster's angle of incidence that direct the beam to the camera (not shown in Fig.1). The near-field images captured by the camera as a function of laser wavelength are analyzed with a computer.

We first studied a 20 m long 125 μm cladding diameter LMA passive fiber. It had a 20 μm diameter core with a numerical aperture of 0.08. Its refractive index profile was measured by an *IFA-100* index profiler (manufactured by *Interfiber Analysis*) at 1000 nm wavelength. The index profile was used in a scalar model to calculate the fiber modes and their group effective index. The modeling showed that the LP_{01}, LP_{11}, LP_{02}, and LP_{12} HOMs were guided by this fiber.

The multi-mode fiber was spliced to the single-mode output pigtail from the laser. It was arranged in ~25 cm diameter loose coils to prevent any bend induced perturbations that may cause mode scattering. Under these conditions the coupling into the fiber is axisymmetric and therefore only the even LP_{02} HOM was observed at the output. A 20 g weight was placed just downstream of the splice to introduce a discrete non-axisymmetric perturbation that could excite odd modes.

The laser wavelength was scanned and near-field images of the fiber's output end face were captured as a function of laser wavelength. Following the standard S^2 analysis[2,3], the Fourier transform of the spectral interference pattern at each pixel was calculated. The transform gives the Fourier amplitude of the intermodal beats as a function of intermodal group delay.

2.2 Analysis and Results

A sum of the Fourier transforms over all the pixels is shown in Fig. 2(a). The Fourier amplitudes can be related to the relative strengths of the beating modes[2]. We verified that peaks S1, S2, and S3 were also present in separate

measurements on a single mode fiber and were therefore caused by known reflections within our experimental setup – they should therefore be ignored. By analyzing the spatial dependence of the Fourier phase and amplitude at an intermodal group delay point, the phase and energy distribution of the mode contributing at that delay can be reconstructed. Reconstruction of the Fourier phase and intensity images at the narrow peak D reveals that it corresponds to discrete scattering into the LP_{11} mode. This mode is excited at the localized perturbation caused by the weight because it appears only when the weight is introduced.
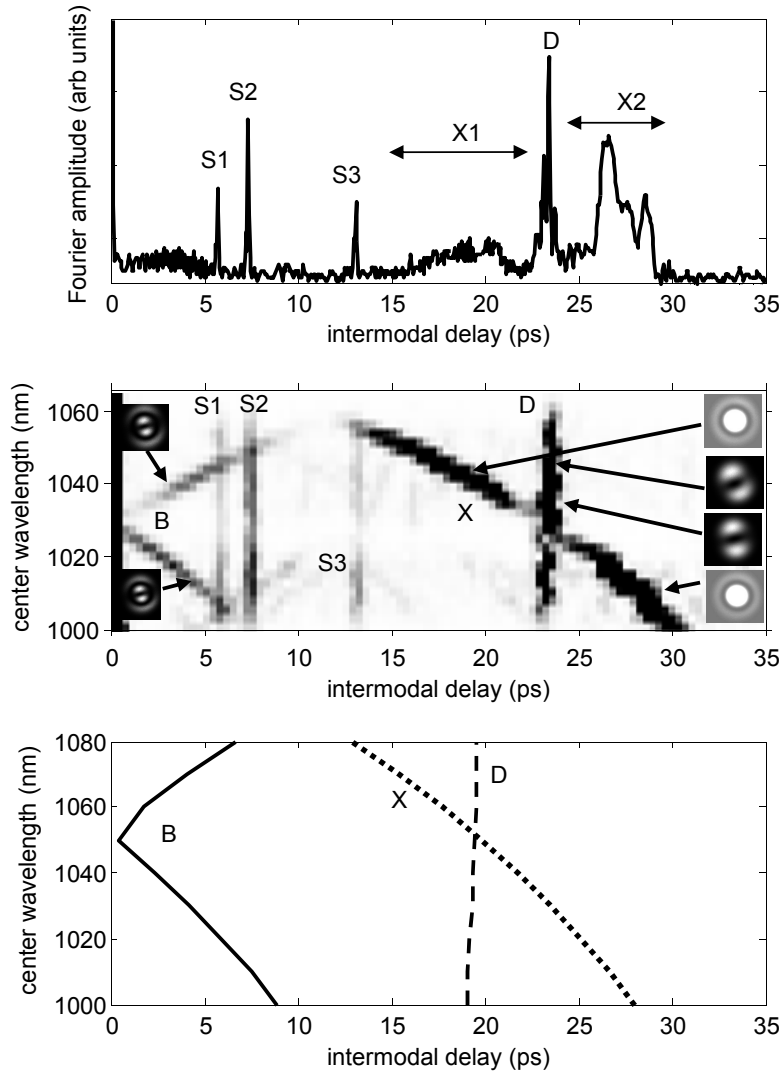

Fig. 2: S^2 data analysis for the LMA fiber using, (a) standard analysis[2,3], and (b) new spectrogram analysis showing a false color representation of variation in intermodal group delay as a function of wavelength. Insets in (b) show the retrieved mode intensity distribution at certain delay and wavelength values. (c) Simulated intermodal group delay as a function of wavelength.

Figure 2(a) also shows a broad distribution in intermodal group delay over regions X1 and X2. Reconstruction of the Fourier phase and intensity over these regions shows that it substantially consists of the LP_{02} mode. According to the standard S^2 interpretation[2-4], these broadened delay distributions X1 and X2 show light coupling from the LP_{01} to the LP_{02} mode over a long length, *i.e.* the fiber causes distributed scattering from the LP_{01} mode into the LP_{02} mode. This interpretation overlooks the group delay dispersion that is often substantial near the mode cutoff of HOMs and therefore falsely identifies the fiber or its fixturing as the excitation source of the HOM.

The dispersion and distributed scattering effects are decoupled by our new analysis method. The S^2 data is collected as above. However when analyzing the data, we take a narrow wavelength window and sweep it across the full laser

spectrum in small wavelength steps. In each wavelength window, the Fourier transforms at all pixels are summed (just as in conventional S^2 analysis). The Fourier transforms of all the windows are stacked together to form a two-dimensional image that shows the Fourier amplitude (in false color) as a function of the intermodal group delay on one axis and the center wavelength of the window on the other axis. We call this two-dimensional image a *spectrogram*. Figure 2(b) shows such a spectrogram recorded with the LMA fiber. We used ~8 nm wide spectral windows with a step size of 2 nm. The spectral width is chosen so that the peaks are resolved in intermodal group delay whereas the step size is chosen to capture the wavelength-dependence of the spectrogram features. The MPI within each wavelength window can be calculated according to the algorithm in Ref.[2] for a wavelength-dependent MPI. The window parameters do not affect the MPI values.

3. DISCUSSION ON THE SPECTROGRAM

The spectrogram has several interesting features. Most importantly we see that the broad delay features X1 and X2 in Fig. 2(a) appear as a single curved streak X in the spectrogram indicating a strong variation of the intermodal group delay from ~13 ps to ~33 ps across the laser tuning range. The insets in Fig. 2(b) show reconstructions of the intensity profile at a few delays along streak X and indicate an LP_{02} mode. On the other hand the peak D in Fig. 2(a) corresponds to a streak with relatively little variation in delay across the laser tuning range indicating that the LP_{11} mode experiences weak intermodal dispersion. Reconstruction of the LP_{11} mode at a couple of points along streak D are shown as insets in Fig. 2(b). This spectrogram correctly identifies that the spread of LP_{02} intermodal group delay (features X1 and X2 in Fig. 2(a)) is actually caused by intermodal fiber dispersion acting on a discrete scattering event at the input splice rather than distributed scattering in the fiber. The theoretical spectrogram was simulated from the calculated group indices. The wavelength dependence of intermodal group delay features X and D (Fig. 2(c)) show good qualitative agreement with the measured data.

In addition an inflected streak B is present in both the measured and simulated spectrograms (Figs. 2(b) and (c)). Reconstruction of the mode intensity along feature B shows a clear mixture of the LP_{11} and LP_{02} modes (see inset of Fig. 2(b)). Therefore feature B arises from the beating of the LP_{11} mode against the LP_{02} mode and the delay values represent the magnitude of intermodal group delay between these two HOMs as a function of wavelength – this is equivalent to the magnitude of the intermodal group delay difference between the trajectories of streaks X and D. Other faint streaks are visible that represent interaction of the fundamental mode with spurious reflections (peaks S1, S2, and S3) in our setup. Whereas they affect the accuracy of an MPI computation, they are specific to our experimental apparatus and are not a fundamental limitation of the spectrogram analysis.

4. SIGNATURE OF DISTRIBUTED SCATERRING IN SPECTROGRAM

In order to demonstrate distributed scattering we recorded a spectrogram with the same LMA fiber coiled to a tight ~6 cm diameter (Fig. 3).
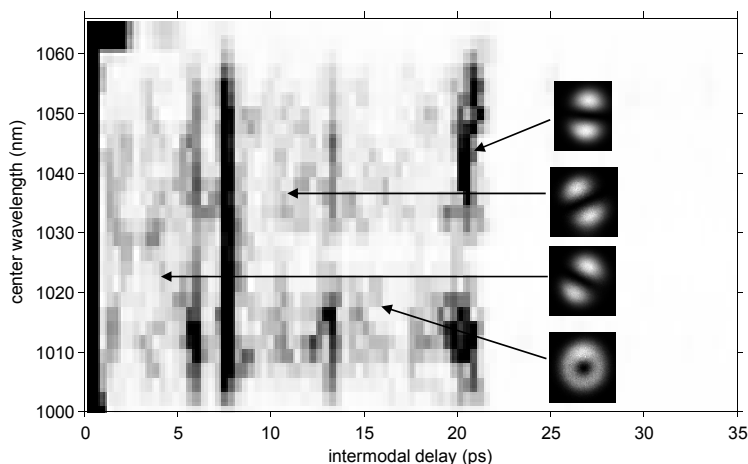

Fig. 3: Spectrogram recorded with the tightly coiled LMA fiber showing distributed scattering. Insets show retrieved mode images at a few representative positions.

The tight coil radius applies a non-axisymmetric index perturbation that couples energy between modes all along the length of the fiber. The spectrogram shows a broad distribution of energy that extends from streak D all the way to zero intermodal group delay, independent of wavelength. Reconstruction of the mode intensity at various delays and wavelengths (Fig. 3 insets) indicates distributed scattering into the LP_{11} mode. Note that the azimuthal orientation of the LP_{11} mode shown in the insets varies more strongly compared to the discrete scattering streak D in Fig. 2(b). At some positions we observe a donut-shaped energy distribution arising from the superposition of different azimuthal orientation of LP_{11} modes. This broad distribution of energy with random mode orientation is a clear signature of distributed scattering along the entire fiber length. Distributed scattering therefore appears as a broad background that has a large spread in intermodal group delay but is relatively independent of wavelength.

5. SPECTROGRAM OF A STANDARD TELECOM SINGLE-MODE FIBER

We also studied a 4.3 m long standard telecom single mode fiber which guides the LP_{01}, and LP_{11} modes at our laser wavelengths. It had some core-cladding eccentricity error which enabled us to excite the LP_{11} mode. The standard S^2 analysis (Fig. 4(a)) shows a broad region M, which would previously have been attributed[2,3] to distributed scattering. However our new spectrogram analysis of this data (Fig. 4(b)) shows that the intermodal group delay across feature M actually varies strongly with wavelength and therefore the delay broadening is due to mode dispersion interacting with discrete scattering into the LP_{11} mode at the input splice.
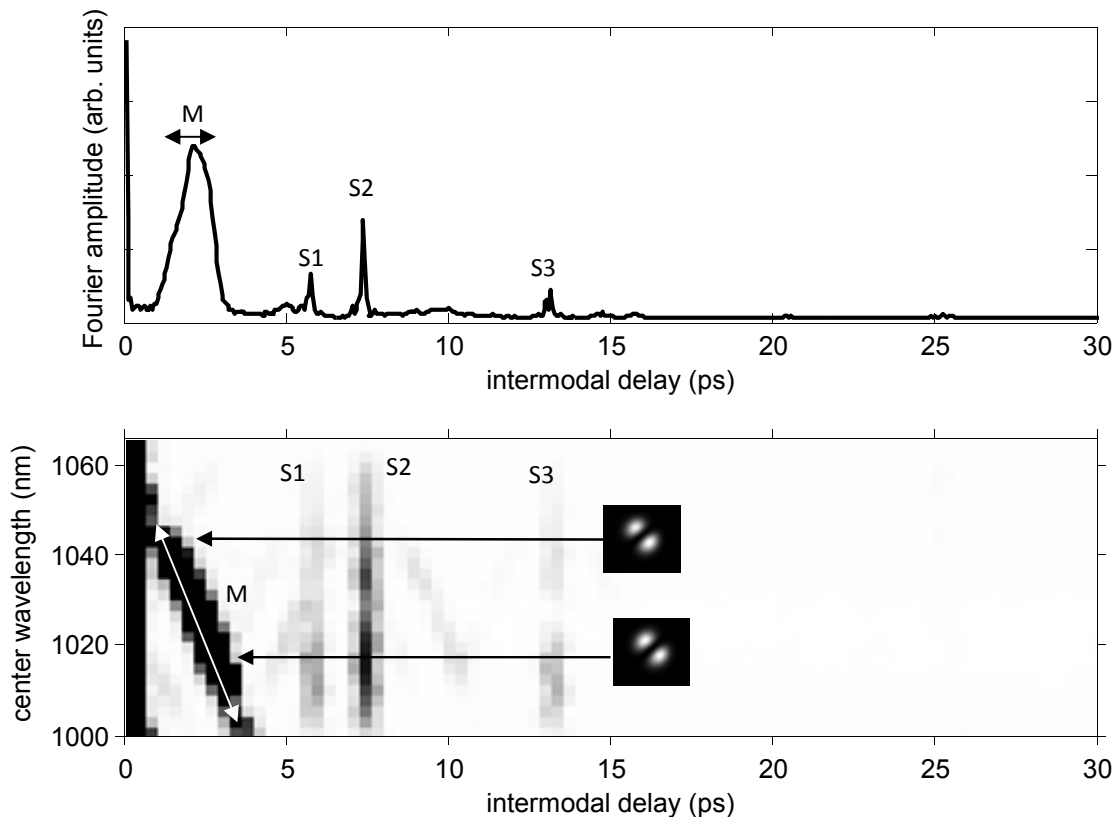

Fig. 4: (a) Standard S^2 analysis, and (b) new spectrogram, analysis of measurements on a standard telecom single mode fiber. Insets in (b) show two representative retrieved mode images.

6. SUMMARY

The effect of intermodal dispersion during the interpretation of S^2 data has been overlooked. But as shown in this paper intermodal dispersion can be significant in few-moded LMA fibers. This dispersion causes a spread or broadening in the features of an S^2 spectrum. The standard one-dimensional representation and interpretation of S^2 data falsely ascribes the spread to distributed scattering in the fiber. The new two-dimensional spectrogram analysis outlined in this paper

distinguishes intermodal dispersion from distributed scattering, overcoming a limitation of the standard one-dimensional representation and interpretation of S^2 data. This new approach is essential for correctly identifying the causes of intermodal scattering in fibers and for evaluating the performance of devices and systems incorporating such fibers.

7. REFERENCES

[1] Wielandy, S., "Implications of higher-order mode content in large mode area fibers with good beam quality", Opt. Express **15**, 15402-15409 (2007).

[2] Nicholson, J.W., Yablon, A.D., Fini, J.M., and Mermelstein, M.D., "Measuring the modal content of Large-Mode-Area Fibers", IEEE J. Sel. Top. In Quantum Electronics **15**, p.61-70 (2009).

[3] Nicholson, J.W., Yablon, A.D., Ramachandran, S., and Ghalmi, S., "Spatially and spectrally resolved imaging of modal content in large-mode-area fibers", Optics Express **16**, p.7233-7243 (2008).

[4] Nguyen, D.M. , Blin, S., Nguyen, T.N., Le, S.D., Provino, L., Thual, M., and Chartier, T., "Modal decomposition technique for multimode fibers", Appl. Opt. **51**, p.450 (2012).

[5] Schimpf, D.N., Barankov, R.A., and Ramachandran, S., "Cross-correlated (C^2) imaging of fiber and waveguide modes," Opt. Express **19**, 13008-13019 (2011).

[6] Bromage, J., Fini, J.M., Dorrer, C., and Zuegel, J.D., "Characterization and optimization of Yb-doped photonic-crystal fiber rod amplifiers using spatially resolved spectral interferometry," Appl. Opt. **50**, 2001-2007 (2011).

[7] Jespersen, K., Li, Z., Gruner-Nielsen, L., Palsdottir, B., Poletti, F., and Nicholson, J.W., "Measuring Distributed Mode Scattering in Long, Few-Moded Fibers," in Optical Fiber Communication Conference, OSA Technical Digest (Optical Society of America, 2012), paper OTh3I.4.

[8] Jasapara, J.C., Andrejco, M.J., DeSantolo, A., Yablon, A.D., Várallyay, Z., Nicholson, J.W., Fini, J.M., DiGiovanni, D.J., Headley, C., Monberg, E., and Dimarcello, F.V., "Diffraction-limited fundamental mode operation of core-pumped very-large-mode-area Er fiber amplifiers", IEEE J. of Selected Topics in Quantum Electronics **15**, 3-11 (2009).

[9] Jasapara, J., and Yablon, A. D., "Spectrogram approach to S^2 fiber mode analysis to distinguish between dispersion and distributed scattering." *Optics Letters* **37**. 3906-3908 (2012).

[10] Nicholson, J.W., Meng, L., Fini, J.M., Windeler, R.S., DeSantolo, A., Monberg, E., DiMarcello, F., Dulashko, Y., Hassan, M., and Ortiz, R, "Measuring higher-order modes in a low-loss, hollow-core, photonic-bandgap fiber", Opt. Express **20**, 20494-20505 (2012).